Journal of Neuroscience Methods 192 (2010) 233–239

Contents lists available at ScienceDirect

Journal of Neuroscience Methods

journal homepage: www.elsevier.com/locate/jneumeth

Staining of fluorogold-prelabeled retinal ganglion cells with calcein-AM: A new method for assessing cell vitality

Philippe Grieshaber[1], Wolf Alexander Lagrèze[1], Christian Noack, Daniel Boehringer, Julia Biermann*

University Eye Hospital Freiburg, Killianstraße 5, 79106 Freiburg im Breisgau, Germany

ARTICLE INFO

Article history:
Received 23 February 2010
Received in revised form 21 July 2010
Accepted 29 July 2010

Keywords:
Retinal ganglion cells
Fluorogold
Retrograde labeling
Apoptosis
Calcein
Retinal whole mount
Quantification

ABSTRACT

Purpose: The number of retinal ganglion cells (RGC) is often used as an outcome measure in neuroprotection. The gold standard for staining RGC is retrograde labeling, e.g. with fluorogold (FG). However, this method alone does not permit to differentiate between viable and dead cells, because dying cells only avoid being counted once they have undergone complete microglial-phagocytosis. To differentiate between viable and dead but still existent RGC, we additionally stained FG-labeled RGC with calcein-acetoxymethylester (CAM).
Methods: The left optic nerves of rats were crushed 6 days after stereotactical injection of FG into both superior colliculi. The right eyes served as controls. Retinal whole mounts were prepared 2, 5, 8 or 11 days after optic nerve crush (ONC), and incubated for 30 min in culture media containing 0.01% CAM. RGC densities were determined in defined areas at different eccentricities under a fluorescence microscope using the appropriate filters. Twice-positive RGC were counted after merging both filters.
Results: The loss of RGC induced by ONC is identified earlier when these cells are detected by FG + CAM rather than by FG-labeling alone. The percentages of FG-positive RGC stained with CAM were 83% in controls, 68% on day 2, 48% on day 5, 26% on day 8, and 9% on day 11 after ONC. The decay rate of FG-prelabeled RGC appears accelerated and becomes more linear when only viable RGC positive for CAM are counted.
Conclusions: The staining of FG-prelabeled RGC with CAM permits the discrimination between dead and viable RGC in retinal whole mounts, which enables to quantify RGC degeneration earlier after injury than by using microglial-phagocytosis-dependant retrograde labeling alone.

1. Introduction

Compared to other neuronal structures in the central nervous system (CNS), the visual system is relatively easy accessible for the examination of degenerative and regenerative processes. Accordingly, retinal ganglion cells (RGC) are often counted to assess the efficacy of various interventions on neuronal damage or the survival in various models of optic nerve injury, e.g. optic nerve crush (ONC) or axotomy (Berkelaar et al., 1994; Isenmann et al., 1997), glaucoma (Hanninen et al., 2002; Lasseck et al., 2007; Quigley, 1999) and ischemia (Jehle et al., 2008a; Jehle et al., 2008b). RGC numbers have been quantified so far by extrapolating from cell counts obtained from representative cross-sections (Fileta et al., 2008; Huang et al., 2006), by determining the proportion of RGC axons in cross-sections of the optic nerve (Levkovitch-Verbin et al., 2003), and by quantifying RGC densities in defined areas of retinal whole mounts (Maeda et al., 2004; Schlamp et al., 2001).

Identifying RGC based on morphologic or size criteria alone cannot completely discriminate between RGC and displaced amacrine cells, which can make up to almost 50% of cells in the ganglion cell layer (GCL) in the rat (Perry, 1981). RGC must therefore be labeled. As conventional immunohistological stains – NeuN (Buckingham et al., 2008; Zhong et al., 2007), neurofilament (Xin et al., 2007), cresyl violet (Lagreze et al., 1999) or apoptotic markers (Harada et al., 2006; Tatton et al., 2001) – do not permit the selective identification of RGC, and Thy-1, which preferentially labels RGC, does not lend itself to quantitative studies of RGC populations in retinal whole mounts (Barnstable and Drager, 1984; Perry et al., 1984), retrograde labeling of RGC became the gold standard technique.

For retrograde labeling, a fluorescent tracer such as fluorogold (FG) (Jehle et al., 2008b; Vidal-Sanz and Lafuente, 2001), DiI (Vidal-Sanz et al., 1988) or 4-Di-10 ASP (Lasseck et al., 2007; Naskar et al., 2002) is injected into the superior colliculus. The axon terminals take up the dye within days and transfer it retrogradely

Abbreviations: CNS, central nervous system; RGC, retinal ganglion cells; ONC, optic nerve crush; FG, fluorogold; CAM, calcein-acetoxymethylester; GCL, ganglion cell layer; AMC, activated microglia cells; +, positive.

* Corresponding author. Tel.: +49 761 270 4001; fax: +49 761 270 4127.
E-mail address: julia.biermann@uniklinik-freiburg.de (J. Biermann).
[1] Both the authors contributed equally to this work.

0165-0270/$ – see front matter © 2010 Elsevier B.V. All rights reserved.
doi:10.1016/j.jneumeth.2010.07.037

into the cell somata in the retina (Schmued and Fallon, 1986; Selles-Navarro et al., 1996). However, there are two shortcomings to this method: (1) it is impossible to assess early postlesional stages because dead fluorogold-positive (FG+) cells do not evade quantification until obvious apoptotic alterations and complete microglia-phagocytosis have occurred and (2) the quantification is increasingly difficult in the advanced stages of cell death because numerous activated microglia cells (AMC) become secondarily FG+ after RGC phagocytosis.

As neuroprotection should both preserve RGC and maintain metabolic function, it seems desirable to obtain additional information on the functional state of RGC after damage and treatment. Recent studies identified Brn3a as an immunological marker to assess RGC-viability after acute optic nerve injury and ocular hypertension (Nadal-Nicolas et al., 2009; Salinas-Navarro et al., 2010). The combination of RGC-specific retrograde labeling and unspecific viability stains could be another approach to assess RGC-viability early after damage. We therefore combined conventional FG-labeling with a cell viability stain using calcein-acetoxymethylester (CAM) in a rat model of ONC. CAM is a membrane-permeable, fluorogenic esterase substrate hydrolyzed intracellularly to a green fluorescent product (calcein). Thus, green fluorescence is an indicator of viable cells. CAM has been used to identify purified RGC in culture (Liu et al., 2007; Otori et al., 1998; Tezel and Yang, 2004), but so far not in retinal whole mounts. In this study, we attempted to quantify viable RGC in whole mounts using FG and CAM as a new method for assessing cell vitality.

2. Materials and methods

2.1. Animals

Adult male and female Sprague–Dawley rats (180–300 g, Charles River, Sulzfeld, Germany) were used in this study. Animals were fed a standard rodent diet *ad libitum* while kept on a 12-h light/12-h dark cycle. All procedures involving animals concurred with the statement of The Association for Research in Vision and Ophthalmology for the use of animals in research, and were approved by the Committee for Animal Welfare of the University of Freiburg. All types of surgery and manipulations were performed under general anesthesia with isoflurane/O_2. Body temperature was maintained at $37 \pm 0.5\,^{\circ}C$ with a heating pad and a rectal thermometer probe. After surgery, Temgesic® (0.05 mg/kg, Essex Pharma, Germany) was applied intraperitoneally to treat pain. While recovering from anesthesia, the animals were placed in separate cages, and gentamicin ointment (Refobacin; Merck, Darmstadt, Germany) was applied on ocular surfaces and skin wounds.

2.2. Retrograde RGC labeling

Deeply anesthetized rats were placed in a stereotactic apparatus (Stoelting, Kiel, Germany), and the skin overlying the skull was cut open and retracted. The lambda and bregma sutures served as landmarks for drilling six holes. We injected 7.8 μl of FG (Fluorochrome, Denver, CO, USA), dissolved in dimethylsulfoxide (FG 3% in NaCl with 10% DMSO), into both superior colliculi as described previously (Jehle et al., 2008b). To ensure adequate RGC labeling, animals were given 6 days to perform the retrograde transport of FG before further experimental intervention.

2.3. Optic nerve crush

The left optic nerve (ON) of rats was approached via orbitotomy on day 7 after stereotactical FG injection into both superior colliculi. After partial removal of the lacrimal gland and transsection of the superior rectus and obliquus muscles, the ON was exposed by blunt dissection of the retractor bulbi muscle. The nerve was separated after splitting the meninges and, as a whole, mechanically crushed directly behind the eyeball for 10 s using a fine forceps without residual aperture. Intact retinal perfusion was confirmed within 3 min after the crush.

2.4. Tissue preparation and CAM staining

Animals were sacrificed by CO_2 inhalation after 2, 5, 8 and 11 days after ONC ($n = 19$). The right, untreated eyes of the animals served as controls. Retinal tissue was immediately harvested and further processed for whole mount preparation in ice-cold Hank's balanced salt solution. Retinae were carefully placed on a nitrocellulose membrane with the GCL on top. After removing the vitreous body, the retinae were incubated in serum-free culture media (Promocell, Heidelberg, Germany) containing 0.01% CAM (Molecular Probes, Inc., Eugene, OR, USA) at 37 °C for 30 min. The preparation–procedure from death to incubation took about 8 min, while the tissue was kept on ice permanently. After incubation, retinae were embedded in mounting media (Vectashield; AXXORA Deutschland, Lörrach, Germany) and immediately recorded. The best staining result was achieved without tissue fixation. However, a short fixation in PFA 4% for 10 min was possible; longer fixation in PFA or fixation in methanol was not possible, as fluorescent calcein easily diffuses through damaged cell membrane over time.

The number of FG+ or CAM+ RGC was further assessed in single labeled retinae of controls and 5 or 8 days after ONC ($n = 3$) and compared with the number of FG+ or CAM+ RGC in twice labeled retinal tissue to exclude a mutual interference of the two dyes.

2.5. Tissue and data analysis

The densities of FG+ and CAM+ RGC were determined in blinded fashion using a fluorescence microscope (AxioImager; Carl Zeiss, Jena, Germany) and the appropriate bandpass emission filters (FG: excitation/emission 331/418 nm; CAM: excitation/emission 495/515 nm). In detail, we photographed three standard rectangular areas (the size thereof was $0.200\,mm \times 0.200\,mm = 0.04\,mm^2$) at 1, 2 and 3 mm from the optic disc in the central regions of each retinal quadrant (Fig. 1A). A picture was recorded after localizing the GCL with the FG filter (Fig. 1B), followed by another picture of the same level in the CAM filter (Fig. 1C). All stained RGC, identified using morphologic criteria, were calculated in each photograph using a cell-counter plugin (dots in Fig. 1A and B, ImageJ software). Thereafter, both counting areas were merged and twice-marked cells (cells with two dots) were then counted (Fig. 1D). Secondary FG-stained AMC after RGC phagocytosis were separated by morphologic criteria and excluded from examination. To acquire cells/mm^2, we multiplied the number of analyzed cells/$0.04\,mm^2$ by 25.

Single labeled retinae (only FG or only CAM labeling) were assessed in a similar manner as described above using the appropriate bandpass emission filter.

Further tissue analysis was achieved with a Leica TCS SP2 AOBS spectral confocal microscope. To determine the depth of CAM-penetration into retinal tissue, retinal whole mounts of controls without FG-labeling were prepared as described above. After CAM staining, retinae were fixed in PFA 4% for 10 min and then embedded in Mowiol embedding medium (Calbiochem, San Diego, CA) containing 4′,6-diamino-2-phenylindole dihydrochloride hydrate (DAPI; Sigma) for nuclear staining. Interestingly, all CAM was incorporated by cells in the inner retina (cells in the GCL, consisting mainly of RGC but also displaced amacrine cells and some

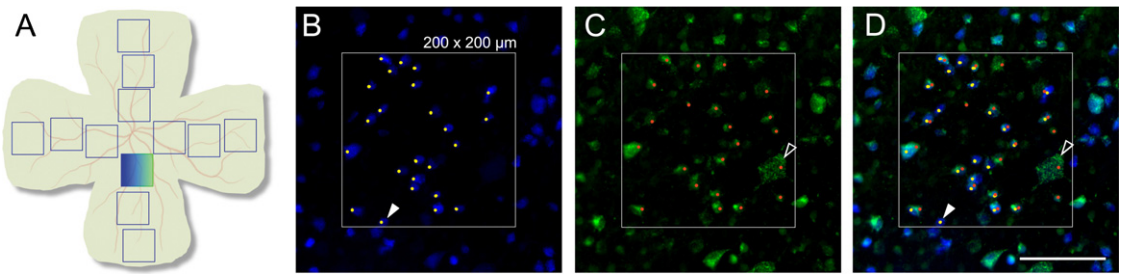

Fig. 1. Method of RGC quantification in the FG and CAM filter. (A) RGC density was determined in three standard rectangular areas per quadrant in both filters (blue: FG, green: CAM). (B and C) Scans of a control retina in the FG (B) and CAM (C) filter. All stained RGC, identified according to morphologic criteria, were marked with a dot and calculated in an area measuring 0.04 mm^2 using a cell-counter plugin (ImageJ software). (D) Thereafter, both counting areas were merged and twice-marked cells (cells with two dots) were additionally counted. Arrowheads accentuate cells which were FG- or CAM-positive. Scale bar in D for all photographs is 100 µm.

endothelial cells). These cells had direct contact to the calcein solution (Fig. 2A). DAPI-positive cells in the inner nuclear layer (INL) (mainly bipolar cells) were not stained by CAM (Fig. 2B). CAM staining infiltrated approximately the upper 5 µm of the retinal whole mount. The external retinal layers, which were covered with the nitrocellulose membrane, were not stained, as shown in a three dimensional reconstruction of the retinal whole mount (Fig. 2C).

2.6. Statistical analysis

All aggregated data are presented as means with their corresponding SEM. Statistical significance was assessed using ANOVA, followed by Tukey–Kramer post hoc testing for multiple comparison procedures. Differences were considered statistically significant at $P < 0.05$. For the survival curves, all RGC densities were normalized to the mean number of FG-labeled control retinae.

3. Results

3.1. CAM labels viable cells in the GCL

Conventional FG-labeling displayed RGC specifically, as shown in Fig. 3A, D and G in representative photographs of a control retina (A–C) and of a retina 2 (D–F) and 8 (G–I) days after ONC. As expected, the number of FG-positive RGC decreased over time after ONC. Calcein was concentrated evenly in the cytoplasm of all viable cells in the GCL (Fig. 3B, E and H), and in retinal vessels (H), whereas the nerve fiber layer was not stained. In conjunction with morphologic characteristics, we identified CAM-positive RGC. The overlay of both filters (Fig. 3C, F and I) allowed the differentia-

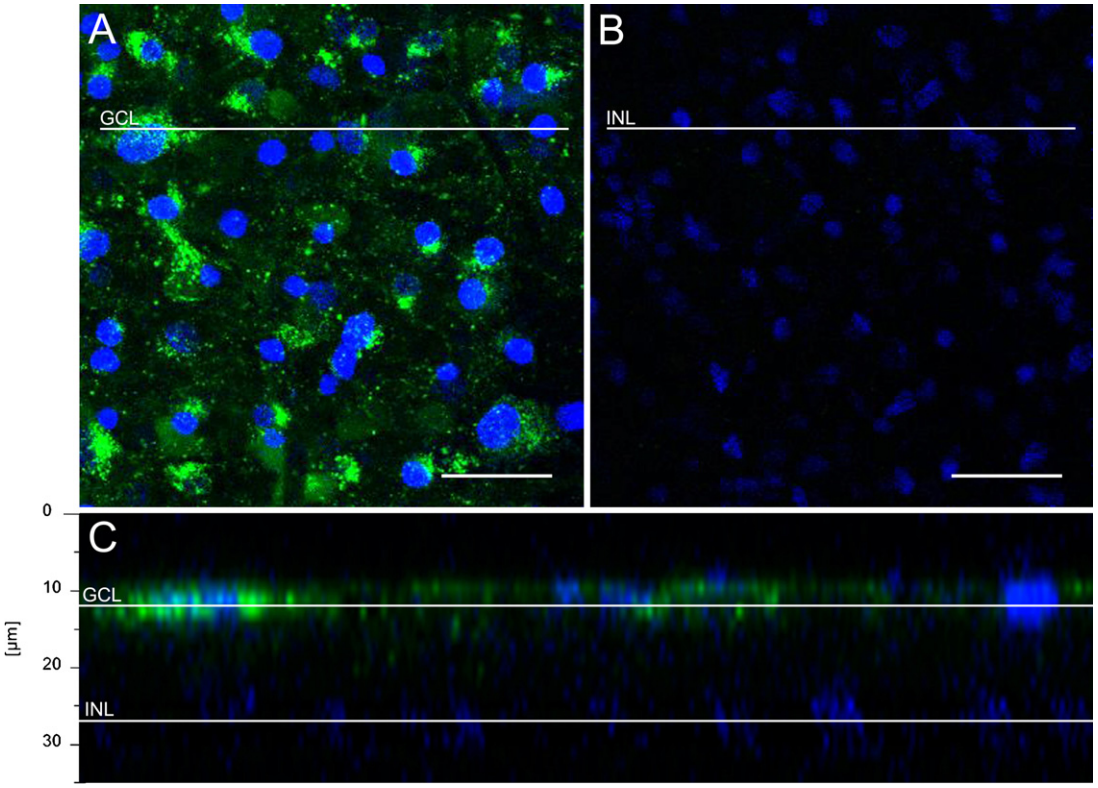

Fig. 2. Confocal microscopy revealed calcein-positive cells only in the GCL. Confocal scans of a flat-mounted retina after CAM staining fixed in PFA 4% for 10 min. Cell nuclei were stained with DAPI. (A) CAM was incorporated by DAPI-positive cells in the GCL, which had direct contact to the calcein solution. (B) DAPI-positive cells in the INL were not stained by CAM. (C) Vertical reconstruction of the whole mount in the location marked in A and B with a white line. CAM staining infiltrated approximately the upper 5 µm of the retinal whole mount. Deeper retinal layers, covered with the nitrocellulose membrane on the bottom, were not stained. Scale bar in A and B 10 µm.

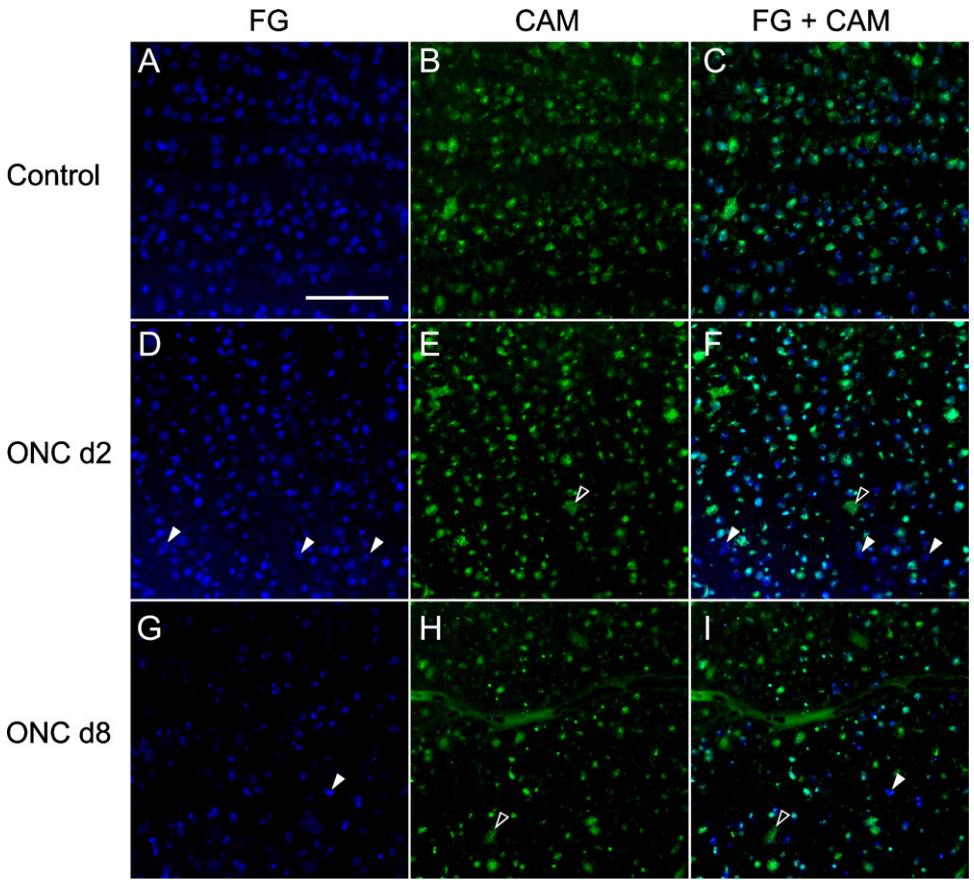

Fig. 3. Twice labeled cells represented viable RGC. Representative photographs of a control retina (A–C) and of a retina 2 (D–F) and 8 (G–I) days after ONC. (A, D and G) Conventional FG-labeling displayed RGC most specifically, whose number decreased over time after ONC. (B, E and H) Calcein stained all viable cells in the GCL and in retinal vessels (H). (C, F and I) The overlay of both filters displayed twice-positive cells, which were thus identified as viable RGC. FG+/CAM− cells (white arrowheads) were most probably dying RGC with preserved morphology not yet cleared by phagocytosis. FG−/CAM+ cells (black arrowheads) were most likely other viable cells in the GCL rather than RGC. Scale bar in I for all photographs is 100 μm.

tion of the following three cell categories: (1) FG+/CAM+ cells were identified as viable RGC, (2) FG+/CAM− cells (white arrowheads), were most probably dying RGC with preserved morphology not yet cleared by phagocytosis, and (3) FG−/CAM+ cells (black arrowheads) were regarded as other viable cells in the GCL rather than RGC.

3.2. Twice labeled cells represented viable RGC

The absolute number of RGC (identified through morphologic criteria and staining) did not differ significantly whether counted in the FG filter or the CAM filter ($P > 0.05$) on any day of analysis. Table 1 presents RGC densities in absolute numbers as means ± SEM. In the controls, RGC densities did not differ significantly when quantified only in the FG filter or in the overlay, as most of the FG+ RGC were CAM+ as well ($P > 0.05$). Two, 5, and 8 days after ONC, RGC densities evaluated in the FG filter or the overlay differed significantly ($P < 0.05$). This might be due to an increasing number of apoptotic RGC, which were still FG+ but inefficient in hydrolyzing CAM to fluorescent calcein. In the later postlesional stages (ONC d11), we observed fewer differences in RGC density (FG versus FG+ CAM, Table 1).

3.3. CAM and FG-labeling do not interfere

To exclude interference of FG and CAM in twice labeled retinae, RGC densities in single labeled retinae of controls and 5 and 8 days after ONC were further examined (Fig. 4). The numbers of FG+ or CAM+ RGC did not differ significantly in single or twice labeled retinal tissue at any day of analysis ($P > 0.05$).

3.4. Twice labeling displayed an almost linear death kinetic of RGC after ONC

The survival curve of RGC is shown in Fig. 5. Normalized to FG-labeled control retinae, 100% of FG-positive RGC were visible on day 2, 79% on day 5, 43% on day 8, and 22% on day 11 after ONC. The percentages of FG-positive RGC stained with CAM were 83% in controls, 68% on day 2, 48% on day 5, 26% on day 8 and 9% on day

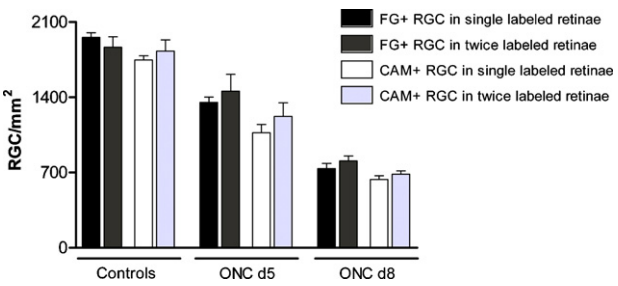

Fig. 4. CAM and FG-labeling do not interfere. The number of FG+ or CAM+ RGC in single labeled retinae of controls and 5 or 8 days after ONC compared with the number of FG+ or CAM+ RGC in twice labeled retinal tissue. The numbers of FG+ or CAM+ RGC (mean ± SEM) did not differ significantly in single or twice labeled retinal tissue at any day of analysis ($P > 0.05$), demonstrating that there is no interference between FG and CAM which could have influenced the quantification.

Table 1
Number of RGC/mm^2 ± SEM in twice labeled retinae that were FG+, CAM+ or both.

	n retinae	FG+	CAM+	FG+ CAM+	P (FG+ vs FG+ CAM+)
Control	6	1866 ± 96	1829 ± 105	1545 ± 73	>0.05
ONC d2	3	1862 ± 96	1711 ± 107	1277 ± 65	<0.01
ONC d5	4	1458 ± 156	1285 ± 109	880 ± 86	<0.05
ONC d8	3	808 ± 47	685 ± 30	491 ± 44	<0.01
ONC d11	3	411 ± 29	527 ± 102	164 ± 8	>0.05

Twelve images per retina were recorded and analyzed. ONC, optic nerve crush; d, day; +, positive; FG, fluorogold; CAM, calcein; vs, versus.

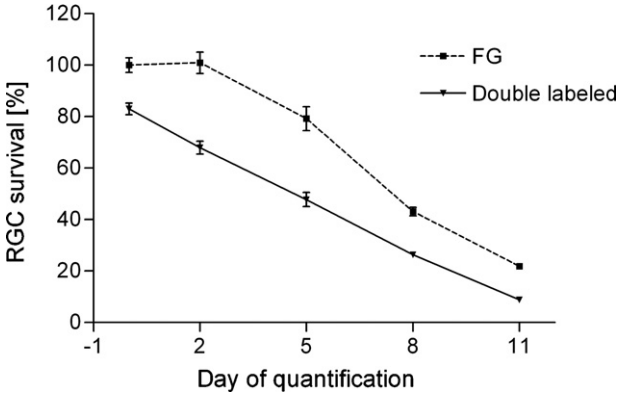

Fig. 5. Survival curve of RGC after ONC. After ONC, the decay rate of prelabeled RGC appears accelerated and becomes more linear when counting only viable RGC positive for CAM as well. Greater deviations in RGC densities were detected between days 2 and 8 after ONC.

11 after ONC. After ONC, the decay rate of prelabeled RGC appears accelerated and becomes more linear (R^2: 0.9985, $P < 0.001$) when counting only viable, CAM+ RGC. Greater deviations in functional RGC stages were detected between day 2 and 8 after ONC.

4. Discussion

Quantification of RGC number in normal and diseased retinal tissue is essential to better understand the mechanisms of RGC death and interventions aiming at neuroprotection. In this investigation we describe a new method for assessing the cell vitality of FG-prelabeled RGC with CAM in whole mounts. This method may permit the discrimination between dead and viable RGC, which enables to quantify RGC degeneration earlier after injury than by using microglial-phagocytosis-dependant retrograde labeling alone.

Adult RGC are widely used as a model to study mechanisms of de- and regeneration within the CNS. All regions of the CNS including the retina share the disadvantage of being composed of heterogeneous populations of cells. In the retina, RGC constitute <1% of the total population (Thanos et al., 2000). Assessments of nerve cell loss based on cell counts and measurements of surviving neurons in the GCL cannot however distinguish with certainty between actual ganglion cells and displaced amacrine cells that may account for nearly half of the neurons in this layer (Cowey and Perry, 1979; Perry, 1981). Thus, specific markers are required to identify subpopulations of retinal neurons in the GCL.

RGC in rodents can be specifically labeled with Thy-1. However, this technique is unsuitable for quantitative studies of RGC populations in retinal whole mounts due to the antibody's insufficient penetration through the internal limiting membrane (Barnstable and Drager, 1984; Perry et al., 1984). Furthermore, Thy-1 expression changes in RGC after injury (Huang et al., 2006). Recently it has been described that RGC in mice and rats can be immunologically detected with antibodies against RGC-specific Brn3a and that Brn3a is downregulated in RGC early after optic nerve transsection or crush, which could make it a well-suitable marker for RGC degeneration in the future (Nadal-Nicolas et al., 2009). However, Brn3a RGC axons have a relative preference for the contralateral hemisphere, RGC that projected ipsilaterally as well as those that project contralaterally to subcortical centers were not Brn3a positive (Quina et al., 2005).

The progress of tracing techniques over the last decades has involved a range of different methodologies, some of which are based on a common principle, namely axonal transport. *In vivo* labeling with fluorescent dyes (FG, Dil, 4-Di-10 ASP) was established, allowing the definition of neuronal populations according to their anatomical connections (Vidal-Sanz et al., 1988). Thus, in this experiment, we used retrograde labeling from the superior colliculus with FG as a specific method to label RGC. The additional CAM staining used in this investigation provided further information about RGC vitality, an important factor in neuroprotection experiments.

At present, there is no adequate substitute for retrograde labeling, although it has some limitations. In animal models, RGC were most commonly labeled retrogradely before a neurodegenerating intervention, and RGC death was assessed by quantifying RGC loss (Fischer et al., 2000; Villegas-Perez et al., 1993). Using this prelabeling technique, one potential source of error is to count dead RGC with preserved morphology that have not yet been cleared by phagocytosis. This drawback, which is particularly relevant within the first 4 days after an intervention, can be circumvented by additional labeling with CAM. By using this method, we did not overestimate the number of RGC of 17%, 33%, 31%, 17% and 13% on days 0, 2, 5, 8, and 11 after ONC, respectively. The 17% difference in control-tissue RGC on day 0 may be due to RGC dying between enucleation and the staining procedure. Another shortcoming of retrograde labeling (with regard to quantification of RGC number) was the phagocytosis-dependent FG-staining of microglia cells. Retrograde and anterograde degeneration have been reported to be sufficient stimuli to activate glial cells which, in turn, are involved in the phagocytosis of dying neurons (Thanos et al., 1994). However, this potential source of error cannot be prevented with CAM; the examiner must still discriminate between different cell types.

An interference of the two dyes could be excluded by the additional examination of single labeled retinae (Fig. 4). Moreover, the two staining methods complement each other due to the following differences: (1) time point and location of labeling (the double-staining of RGC reported here was a combination of an *in vivo* staining with retrogradly transported FG from superior colliculus and additional staining of the retinal flat mount with CAM *in vitro*); (2) mechanism of labeling (FG was retrogradely transported from the RGC axon into the soma prior to ONC (RGC-specific labeling) while CAM penetrates the membranes of the superficial cell layer of the whole mount and was then hydrolyzed intracellularly to green fluorescent calcein (vitality specific labeling)). The different staining pattern of the retinal cells seen in Fig. 3D–I results from these differences and allows to discriminate between viable and dead RGC.

In this set of experiments, we found that 57% or 74% RGC were lost 8 days after ONC using FG alone or FG and CAM, respectively. This concurs in part with previous studies using other techniques for quantifying RGC after ONC. Leung et al. (2008) found fairly similar results (more than 80% at week 1 after ONC) of Thy1-CFP-expressing RGC using a blue-light confocal scanning laser ophthalmoscope in mice. Like our method, the method reported by Leung based to some degree on cell function, as stressed but alive RGC switched off the Thy1-CFP-signal leading to a much higher estimate of RGC loss. By contrast, Higashide et al. (2006) imaged retrogradely-labeled RGC *in vivo* with a scanning laser ophthalmoscope, demonstrating that approximately 30% of RGC were lost by day 7 after ONC, respectively. This obviously much smaller RGC loss may be explained by the following: Higashide et al. just counted bright blobs in blurry retinal images, thus they were not able to distinguish RGC and FG-filled microglia by morphology (false high RGC count). Visualizing apoptosing RGC with intravitreal injection of Annexin 5, Cordeiro et al. reported that 40% of RGC were lost by day 7 and 76% were lost by day 12 after optic nerve transsection (Cordeiro et al., 2004).

Hence, the additional staining of FG-prelabeled RGC with CAM seems to identify viable RGC in the GCL of retinal whole mounts and may help characterize neuroprotective agents more precisely. Using the protocol as stated in this manuscript, all CAM was incorporated by cells in the inner retina (the upper 5 μm of the retinal whole mount, consisting mainly of RGC but also displaced amacrine cells and some endothelial cells). We speculate that the cells of the inner retina act as a barrier which, to some degree, prevents diffusion of CAM into the outer retina. After transport into the cells, intracellular esterases remove the acetomethoxy group, the calcein molecule gets trapped inside and develops a strong green fluorescence. Thus, penetration into deeper layers may not be possible. The outer/external retinal layers were not stained by CAM, as they were covered with the nitrocellulose membrane which seems to be an insuperable barrier for CAM. The CAM staining procedure is easy to implement, although longer fixation of retinal whole mounts with PFA or methanol after CAM labeling is not recommended (fluorescent calcein can diffuse through damaged cell membranes). Short fixation in 4% PFA for 10 min is possible when the retinal tissue is photographed immediately afterwards. Furthermore, the quality of the CAM staining in whole mounts was weaker compared to the staining result achieved for single neurons in culture reported elsewhere (Liu et al., 2007; Otori et al., 1998; Tezel and Yang, 2004). Interestingly, RGC-dendrites and -axons are not markedly stained by CAM in whole mounts, which seems to be an advantage when counting viable RGC. In experiments addressing interventions interfering with neuronal survival, improved accuracy and feasibility of RGC quantification using flat mounts would have been achieved by quantifying the whole flat mount (Danias et al., 2002) instead of random testing of 12 locations distributed in 3 eccentricities and 4 quadrants. However, the special software tool used by Danias et al. may not be available for some scientists.

Acknowledgements

The authors would like to thank Mrs. Sylvia Zeitler for excellent technical assistance, and Dr. Marie Follo, Core Facility – University Hospital Freiburg, for help with confocal microscopy. Grant information: J.B. was supported by the Forschungskommission des Universitätsklinikums Freiburg and the Deutsche Ophthalmologische Gesellschaft.

References

Barnstable CJ, Drager UC. Thy-1 antigen: a ganglion cell specific marker in rodent retina. Neuroscience 1984;11:847–55.
Berkelaar M, Clarke DB, Wang YC, Bray GM, Aguayo AJ. Axotomy results in delayed death and apoptosis of retinal ganglion cells in adult rats. J Neurosci 1994;14:4368–74.
Buckingham BP, Inman DM, Lambert W, Oglesby E, Calkins DJ, Steele MR, et al. Progressive ganglion cell degeneration precedes neuronal loss in a mouse model of glaucoma. J Neurosci 2008;28:2735–44.
Cordeiro MF, Guo L, Luong V, Harding G, Wang W, Jones HE, et al. Real-time imaging of single nerve cell apoptosis in retinal neurodegeneration. Proc Natl Acad Sci USA 2004;101:13352–6.
Cowey A, Perry VH. The projection of the temporal retina in rats, studied by retrograde transport of horseradish peroxidase. Exp Brain Res 1979;35:457–64.
Danias J, Shen F, Goldblum D, Chen B, Ramos-Esteban J, Podos SM, et al. Cytoarchitecture of the retinal ganglion cells in the rat. Invest Ophthalmol Vis Sci 2002;43:587–94.
Fileta JB, Huang W, Kwon GP, Filippopoulos T, Ben Y, Dobberfuhl A, et al. Efficient estimation of retinal ganglion cell number: a stereological approach. J Neurosci Methods 2008;170:1–8.
Fischer D, Pavlidis M, Thanos S. Cataractogenic lens injury prevents traumatic ganglion cell death and promotes axonal regeneration both in vivo and in culture. Invest Ophthalmol Vis Sci 2000;41:3943–54.
Hanninen VA, Pantcheva MB, Freeman EE, Poulin NR, Grosskreutz CL. Activation of caspase 9 in a rat model of experimental glaucoma. Curr Eye Res 2002;25:389–95.
Harada C, Nakamura K, Namekata K, Okumura A, Mitamura Y, Iizuka Y, et al. Role of apoptosis signal-regulating kinase 1 in stress-induced neural cell apoptosis in vivo. Am J Pathol 2006;168:261–9.
Higashide T, Kawaguchi I, Ohkubo S, Takeda H, Sugiyama K. In vivo imaging and counting of rat retinal ganglion cells using a scanning laser ophthalmoscope. Invest Ophthalmol Vis Sci 2006;47:2943–50.
Huang W, Fileta J, Guo Y, Grosskreutz CL. Downregulation of Thy1 in retinal ganglion cells in experimental glaucoma. Curr Eye Res 2006;31:265–71.
Isenmann S, Wahl C, Krajewski S, Reed JC, Bahr M. Up-regulation of Bax protein in degenerating retinal ganglion cells precedes apoptotic cell death after optic nerve lesion in the rat. Eur J Neurosci 1997;9:1763–72.
Jehle T, Dimitriu C, Auer S, Knoth R, Vidal-Sanz M, Gozes I, et al. The neuropeptide NAP provides neuroprotection against retinal ganglion cell damage after retinal ischemia and optic nerve crush. Graefes Arch Clin Exp Ophthalmol 2008a;246:1255–63.
Jehle T, Wingert K, Dimitriu C, Meschede W, Lasseck J, Bach M, et al. Quantification of ischemic damage in the rat retina: a comparative study using evoked potentials, electroretinography, and histology. Invest Ophthalmol Vis Sci 2008b;49:1056–64.
Lagreze WA, Otto T, Feuerstein TJ. Neuroprotection in ischemia of the retina in an animal model. Ophthalmologe 1999;96:370–4.
Lasseck J, Schroer U, Koenig S, Thanos S. Regeneration of retinal ganglion cell axons in organ culture is increased in rats with hereditary buphthalmos. Exp Eye Res 2007;85:90–104.
Leung CK, Lindsey JD, Crowston JG, Lijia C, Chiang S, Weinreb RN. Longitudinal profile of retinal ganglion cell damage after optic nerve crush with blue-light confocal scanning laser ophthalmoscopy. Invest Ophthalmol Vis Sci 2008;49:4898–902.
Levkovitch-Verbin H, Quigley HA, Martin KR, Zack DJ, Pease ME, Valenta DF. A model to study differences between primary and secondary degeneration of retinal ganglion cells in rats by partial optic nerve transection. Invest Ophthalmol Vis Sci 2003;44:3388–93.
Liu Q, Ju WK, Crowston JG, Xie F, Perry G, Smith MA, et al. Oxidative stress is an early event in hydrostatic pressure induced retinal ganglion cell damage. Invest Ophthalmol Vis Sci 2007;48:4580–9.
Maeda K, Sawada A, Matsubara M, Nakai Y, Hara A, Yamamoto T. A novel neuroprotectant against retinal ganglion cell damage in a glaucoma model and an optic nerve crush model in the rat. Invest Ophthalmol Vis Sci 2004;45:851–6.
Nadal-Nicolas FM, Jimenez-Lopez M, Sobrado-Calvo P, Nieto-Lopez L, Canovas-Martinez I, Salinas-Navarro M, et al. Brn3a as a marker of retinal ganglion cells: qualitative and quantitative time course studies in naive and optic nerve-injured retinas. Invest Ophthalmol Vis Sci 2009;50:3860–8.
Naskar R, Wissing M, Thanos S. Detection of early neuron degeneration and accompanying microglial responses in the retina of a rat model of glaucoma. Invest Ophthalmol Vis Sci 2002;43:2962–8.
Otori Y, Wei JY, Barnstable CJ. Neurotoxic effects of low doses of glutamate on purified rat retinal ganglion cells. Invest Ophthalmol Vis Sci 1998;39:972–81.
Perry VH. Evidence for an amacrine cell system in the ganglion cell layer of the rat retina. Neuroscience 1981;6:931–44.
Perry VH, Morris RJ, Raisman G. Is Thy-1 expressed only by ganglion cells and their axons in the retina and optic nerve? J Neurocytol 1984;13:809–24.
Quigley HA. Neuronal death in glaucoma. Prog Retin Eye Res 1999;18:39–57.
Quina LA, Pak W, Lanier J, Banwait P, Gratwick K, Liu Y, et al. Brn3a-expressing retinal ganglion cells project specifically to thalamocortical and collicular visual pathways. J Neurosci 2005;25:11595–604.
Salinas-Navarro M, Alarcon-Martinez L, Valiente-Soriano FJ, Jimenez-Lopez M, Mayor-Torroglosa S, Aviles-Trigueros M, et al. Ocular hypertension impairs optic nerve axonal transport leading to progressive retinal ganglion cell degeneration. Exp Eye Res 2010;90:168–83.
Schlamp CL, Johnson EC, Li Y, Morrison JC, Nickells RW. Changes in Thy1 gene expression associated with damaged retinal ganglion cells. Mol Vis 2001;7:192–201.
Schmued LC, Fallon JH. Fluoro-Gold: a new fluorescent retrograde axonal tracer with numerous unique properties. Brain Res 1986;377:147–54.

Selles-Navarro I, Villegas-Perez MP, Salvador-Silva M, Ruiz-Gomez JM, Vidal-Sanz M. Retinal ganglion cell death after different transient periods of pressure-induced ischemia and survival intervals. A quantitative in vivo study. Invest Ophthalmol Vis Sci 1996;37:2002–14.

Tatton NA, Tezel G, Insolia SA, Nandor SA, Edward PD, Wax MB. In situ detection of apoptosis in normal pressure glaucoma. A preliminary examination. Surv Ophthalmol 2001;45(Suppl. 3):S268–72 (discussion S73–6).

Tezel G, Yang X. Caspase-independent component of retinal ganglion cell death, in vitro. Invest Ophthalmol Vis Sci 2004;45:4049–59.

Thanos S, Fischer D, Pavlidis M, Heiduschka P, Bodeutsch N. Glioanatomy assessed by cell-cell interactions and phagocytotic labelling. J Neurosci Methods 2000;103:39–50.

Thanos S, Kacza J, Seeger J, Mey J. Old dyes for new scopes: the phagocytosis-dependent long-term fluorescence labelling of microglial cells in vivo. Trends Neurosci 1994;17:177–82.

Vidal-Sanz M, Lafuente MP, Mayor S, de Imperial JM, Villegas-Perez MP. Retinal ganglion cell death induced by retinal ischemia. Neuroprotective effects of two alpha-2 agonists. Surv Ophthalmol 2001;45(Suppl. 3):S261–7 (discussion S73–6).

Vidal-Sanz M, Villegas-Perez MP, Bray GM, Aguayo AJ. Persistent retrograde labeling of adult rat retinal ganglion cells with the carbocyanine dye dil. Exp Neurol 1988;102:92–101.

Villegas-Perez MP, Vidal-Sanz M, Rasminsky M, Bray GM, Aguayo AJ. Rapid and protracted phases of retinal ganglion cell loss follow axotomy in the optic nerve of adult rats. J Neurobiol 1993;24:23–36.

Xin H, Yannazzo JA, Duncan RS, Gregg EV, Singh M, Koulen P. A novel organotypic culture model of the postnatal mouse retina allows the study of glutamate-mediated excitotoxicity. J Neurosci Methods 2007;159:35–42.

Zhong L, Bradley J, Schubert W, Ahmed E, Adamis AP, Shima DT, et al. Erythropoietin promotes survival of retinal ganglion cells in DBA/2J glaucoma mice. Invest Ophthalmol Vis Sci 2007;48:1212–8.